Frontiers in Bioscience Landmark

Front. Biosci. (Landmark Ed) **2025**; 30(5): 38078
https://doi.org/10.31083/FBL38078

Original Research

Trimethylamine N-oxide Supplementation Enhances the Quality of Oocytes in Mice of Polycystic Ovary Syndrome

Jiayu Huang[1,2,3,†], Yin Tian[2,†], Xuemei Liu[2,4], Zixin Xu[5], Chong Li[2], Ling Zhu[2], Xiru Liu[1], Jiying Hou[6,*], Jingyu Li[2,*]

[1]Reproductive Medicine Center, The First Affiliated Hospital of Chongqing Medical University, 400016 Chongqing, China
[2]Chongqing Key Laboratory of Human Embryo Engineering and Precision Medicine, NHC Key Laboratory of Birth Defects and Reproductive Health, Center for Reproductive Medicine, Chongqing Health Center for Women and Children, Women and Children's Hospital of Chongqing Medical University, 400016 Chongqing, China
[3]The Chongqing Key Laboratory of Translational Medicine in Major Metabolic Diseases, The First Affiliated Hospital of Chongqing Medical University, 400016 Chongqing, China
[4]Molecular Biology Laboratory of Respiratory Disease, Key Laboratory of Clinical Laboratory Diagnostics (Ministry of Education), College of Laboratory Medicine, Chongqing Medical University, 400016 Chongqing, China
[5]Department of Obstetrics and Gynecology, Faculty of Medicine, The University of Tokyo, 113-8655 Tokyo, Japan
[6]Faculty of Basic Medical Sciences, Chongqing Medical and Pharmaceutical College, 401331 Chongqing, China
*Correspondence: houjiying@hotmail.com (Jiying Hou); cqtnljy@gmail.com (Jingyu Li)
[†]These authors contributed equally.

Academic Editor: Indrajit Chowdhury
Submitted: 14 February 2025 Revised: 27 March 2025 Accepted: 7 April 2025 Published: 22 May 2025

Abstract

Background: Polycystic ovary syndrome (PCOS) has increasingly emerged as a significant cause of impaired reproductive outcomes, primarily characterized by a combination of ovulatory dysfunction and decreased oocyte quality. However, the molecular mechanisms underlying the decreased oocyte quality caused by PCOS and preventative strategies still require further investigation. **Method**: All procedures were approved by the Animal Ethics Committee of Chongqing Medical University. We established a mice model of PCOS using dehydroepiandrosterone (DHEA) treatment. The estrous cycle was recorded, and plasma sex hormone and trimethylamine N-oxide (TMAO) levels were measured. Ovarian indices and follicular formation were compared. Time-lapse imaging was used to observe *in vitro* maturation and blastocyst formation. Reactive oxygen species (ROS), MitoSOX level, and mitochondrial membrane potential were measured to analyze the mitochondrial function of oocytes. Confocal laser scanning microscopy was used to detect spindle function and chromosomes. **Results**: Our study found that DHEA-induced PCOS mice exhibited significantly lower plasma TMAO levels compared to normal mice. Consequently, we supplemented TMAO in PCOS mice and found that the abnormal estrous cycle and reduced ovarian function induced by PCOS could be restored. Additionally, TMAO rescued PCOS-induced defects in oocyte maturation, spindle and chromosome morphology, and embryonic developmental potential. Mechanically, we found that TMAO effectively reduced ROS levels by improving mitochondrial function in PCOS oocytes. **Conclusion**: Our findings indicate that the reduction in TMAO levels induced by PCOS may be a key factor influencing reproductive outcomes. TMAO supplementation *in vivo* can effectively enhance mitochondrial function and oocyte quality in PCOS, holding significant clinical importance for improving assisted reproductive outcomes in patients with PCOS.

Keywords: polycystic ovary syndrome; trimethylamine; reactive oxygen species; oocytes; dehydroepiandrosterone; mitochondria

1. Introduction

Polycystic ovary syndrome (PCOS) is a widespread endocrine and metabolic disorder in women, affecting about 20% of the female population in some areas, with an increasing prevalence [1,2]. Commonly, patients exhibit symptoms such as hyperandrogenemia, obesity, and insulin resistance along with impaired ovulation, scanty menstruation, and even amenorrhea [3,4]. Due to ovulatory dysfunction, patients with PCOS frequently rely on assisted reproductive technology (ART) to conceive [5]. Several studies have shown a significant correlation between PCOS and reduced diversity of the gut microbiome. This phenomenon is associated with changes in the composition of substances in the follicular fluid, which are related to the structural characteristics of the flora [6,7].

The intestinal flora is involved in various human metabolic processes. Alterations in the composition of the intestinal flora result in changes in the concentrations of metabolites such as bile acids, short-chain fatty acids (SCFAs), and trimethylamine N-oxide (TMAO), which may lead to several abnormalities [8]. TMAO, a metabolite of choline, primarily forms when gut bacteria catalyze the conversion of choline to trimethylamine, which is then absorbed and rapidly oxidized to TMAO by flavin-containing monooxygenase 3 (FMO3) in the liver [9,10]. Red meat, eggs, dairy products, and saltwater fish are rich in choline,

lecithin, and L-carnitine, all of which are potential food sources of TMAO. As a choline-derived metabolite, TMAO is a key component of biofilms, which plays a vital role in follicular development and oocyte maturation [11,12].

PCOS patients typically exhibit systemic oxidative stress, including in follicular fluid, owing to metabolic dysregulation [13,14]. This oxidative stress is intricately linked to a cascade of adverse reproductive outcomes: declining oocyte quality, reduced fertilization rates, compromised embryo quality, and lower pregnancy rates, thereby significantly impairing pregnancy outcomes. Elevated oxidative stress products induce oocyte apoptosis by disrupting intracellular mitochondrial function and glucose metabolism, resulting in oocyte damage [15,16]. Thus, improving oocyte mitochondrial function and mitigating oxidative stress are pivotal for optimizing pregnancy outcomes in PCOS.

In this study, we established a PCOS mouse model using dehydroepiandrosterone (DHEA) treatment and found significantly decreased plasma TMAO levels. We explored the role of TMAO in DHEA-induced PCOS mice and found that TMAO supplementation could significantly improve mitochondrial function in PCOS oocytes, thereby enhancing oocyte maturation and developmental potential.

2. Materials and Methods

2.1 Animal and Experimental Grouping

All procedures were approved by the Animal Ethics Committee of Chongqing Medical University (Approval No. IACUC-CQMU-2023-0152; Chongqing, China). Four-week-old Institute of Cancer Research (ICR) mice were obtained from Charles River Co. (Beijing, China). The mice were maintained at a controlled temperature of 20–23 °C under a 12/12-h light/dark cycle, with free access to food and water throughout the study period. As shown in Fig. 1A, female mice weighing 22–24 g were randomly assigned to four groups: Normal control (NC), PCOS, PCOS+TMAO (P+T), and TMAO groups. Mice in the NC group were subcutaneously injected with corn oil for 21 consecutive days. The PCOS group received a daily subcutaneous injection of DHEA (S6278; Selleck Chemicals, Houston, TX, USA) at a dose of 6 mg/100 g body weight, dissolved in corn oil, for 21 days. The P+T group received a daily subcutaneous injection of DHEA and were fed TMAO (0.12% dissolved in ddH2O, 317594; Sigma-Aldrich, Darmstadt, Germany) for 30 days. The dose of TMAO was derived from a previous study [17]. The TMAO group was fed TMAO for 4 weeks and received subcutaneous injections of corn oil for 21 consecutive days. Throughout the experimental period, female mice were weighed once a week. At the end of the modeling process (including ovulation induction treatment), experimental mice were anesthetized deeply by intraperitoneal injection of 3% pentobarbital at a dosage of 50 mg/kg and then mice followed by execution with high concentrations of carbon dioxide. The euthanasia method is detailed in the **Supplementary Material**.

2.2 Liquid Chromatography–Tandem Mass Spectrometry

Liquid chromatography–tandem mass spectrometry (LC-MS/MS; ACQUITY UPLC H Class/Xevo G2 TQ-XS MS/MS; Waters Co., Milford, MA, USA) was used for quantification of plasma testosterone, DHEA, and TMAO by Metabo-Profile Biotechnology (Shanghai, China). The plasma samples were thawed under an ice bath. Then 50 µL sample was added to a 1.5 mL centrifuge tube, after which 50 µL deuterium-labeled acetonitrile solution was added, followed by 1 mL methyl tertiary butyl ether. The tube was shaken vigorously for 30 s (Vortex-Genie model 2; Scientific Industries; Bohemia, NY, USA) and centrifuged at a high speed for 10 min at 18,000 g (Microfuge 20R; Beckman Coulter, Inc., Indianapolis, IN, USA). After centrifugation, all supernatants were transferred to a 1.5 mL centrifuge tube, dried under nitrogen at 60 °C, and reconstituted with 70 µL of 20% methanol solution. Then the target compounds were detected with LC-MS/MS. The column parameters were ACQUITY UPLC BEH C18 1.7 µM analytical column (2.1 × 100 mm). Detection mobile phase was: A = water (2% methanol water containing 0.1% formic acid); B = 0.1% formic acid methanol. Elution conditions were: 0–3.5 min (43% B), 3.5–4 min (43–46% B), 4–9.5 min (46–85% B), 9.5–9.8 min (85–100% B), 9.8–12 min (100% B), 12–15 min (100–43% B).

2.3 Estrous Cycle

The normal estrous cycle in mice, consisting of proestrus, estrus, metestrus, and diestrus, spans 4–5 days and was determined through microscopic examination of vaginal cells (ECLipse-Ti2U, Nikon, Tokyo, Japan). Vaginal cells were collected daily from the vaginal with a small amount of sterile saline and evenly dispersed onto glass slides. After the slides partially dried, they underwent Pap was stained. Then the stage of the estrous cycle for each group of mice was determined by analyzing the ratio of epithelial cells, keratinocytes, and leukocytes. The PCOS model was considered successful if the mice exhibited keratinization of the vaginal epithelial cells for seven consecutive days.

2.4 Histological Analyses of Ovaries

After the ovarian tissues were removed, they were fixed in a 10-fold volume of 4% paraformaldehyde (PFA) (pH 7.5) (G1101; Servicebio, Wuhan, China). After fixation for more than 1 week, the tissues were dehydrated with alcohol and embedded in paraffin. Then the embedded tissues were serially sectioned to a thickness of 50 µm. At least five consecutive sections were taken and stained with hematoxylin and eosin (H&E). The sections were sealed with neutral resin at the end of staining. At least two ovaries from four mice were analyzed in each group.

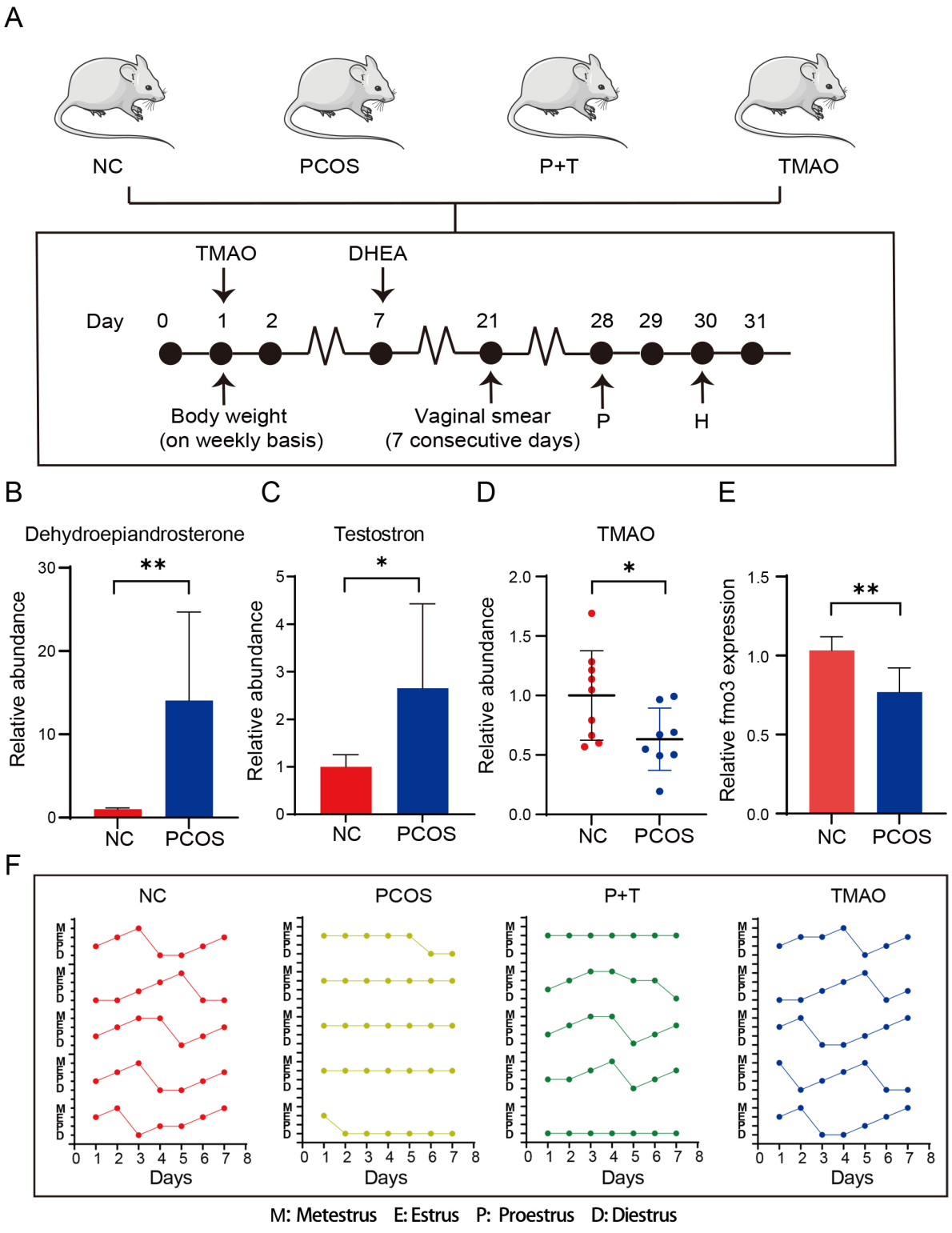

Fig. 1. Establishment of mouse model. (A) Timeline of DHEA and TMAO administration. (B) The relative dehydroepiandrosterone level of PCOS (n = 8) and NC group (n = 8). (C) The relative testosterone level of PCOS (n = 8) and NC group (n = 8). (D) The relative plasma TMAO level of PCOS (n = 9) and NC groups (n = 8). (E) The relative FMO3 expression level of PCOS (n = 3) and NC group (n = 3). (F) The estrous cycle of the NC (n = 7); PCOS (n = 7); P+T group (n = 10) and TMAO group (n = 7). The dot indicates the position of estrous cycle through daily vaginal smear. Data are means ± SEM of at least three independent experiments. *$p < 0.05$, **$p < 0.01$. DHEA, dehydroepiandrosterone; TMAO, trimethylamine N-oxide; PCOS, Polycystic ovary syndrome; NC, Normal control; FMO3, flavin-containing monooxygenase 3; SEM, standard error of the mean; PMSG, pregnant mare serum gonadotropin; hCG, human chorionic gonadotrophin; P+T, PCOS+TMAO.

2.5 Oocyte Collection and Culture

Following superovulation treatment in mice, cumulus-oocyte complexes (COCs) were collected. Separation of oocytes was performed using specialized glass pipettes under stereomicroscopic guidance (SMZ1270, Nikon, Tokyo, Japan). Oocytes and embryos were scored using morphological methods. Laboratory conditions and criteria of oocytes and embryos included in the study were based on the ESHER guidelines [18]. All procedures were performed under sterile conditions. Routine mycoplasma PCR testing was performed to ensured that the oocytes and embryo was free of mycoplasma contamination.

Mice were injected intraperitoneally with 10 IU pregnant mare serum gonadotropin (PMSG). After intervention, mice were euthanized for the collection of germinal vesicles (GV) stage oocytes. The ovaries were isolated and placed in the collection solution. The follicles were punctured with a hypodermic needle to release GV stage oocytes. Then these oocytes were washed several times, transferred to a petri dish containing M16 medium (MR-016; Sigma, St. Louis, MO, USA), and placed in the EmbryoScope™ time-lapse imaging system (Vitrolife AB, Gothenburg, Sweden) at 37 °C with 5% carbon dioxide (CO_2). After 14–16 h of *in vitro* maturation (IVM), metaphase II (MII) stage oocytes were selected for subsequent experiments using an incubation microscope (SMZ1270, Nikon, Tokyo, Japan).

To collect MII stage oocytes, mice were injected intraperitoneally with 5 IU PMSG for superovulation, followed by 5 IU human chorionic gonadotrophin (hCG) 48 h later. Cumulus-oocyte complexes were collected from the oviductal ampulla, and cumulus cells were removed using 0.2% hyaluronidase (P811, Sigma-Aldrich, St. Louis, MO, USA). Then healthy MII oocytes were collected for subsequent experiments. In the embryology part of the experiment, spermatozoa were collected from adult male ICR mice and cultured in Human Tubal Fluid (HTF) medium (MR-070-D; Sigma-Aldrich, St. Louis, MO, USA) for 1 h. MII oocytes were incubated with sperm for 6 h at 37 °C in a humidified environment with 5% CO_2. The sperm concentration for fertilization was 1×10^6/mL. Two-cell embryos were cultured in potassium-supplemented simplex optimized medium (KSOM, MR-101-D; Sigma-Aldrich, St. Louis, MO, USA), and the processes of fertilization, cleavage, and blastocyst formation were carried out in KSOM.

2.6 Immunofluorescence and Confocal Microscopy

0.1% polyvinyl alcohol (PVA) was used to make a phosphate-buffered saline (PBS)-PVA mixture. Then 4% PFA and 0.5% Triton X-100 was formulated from PBS-PVA. Oocytes were fixed in 4% PFA for 20 min and permeabilized in 0.5% Triton X-100 for 20 min. Then oocytes were blocked in a 3% bovine serum albumin (BSA) solution for 1 h (A5256701, Thermo Fisher Scientific, Waltham, MA, USA), incubated overnight at 4 °C with an anti-α-tubulin fluorescein isothiocyanate antibody (F2168, Sigma-Aldrich, St. Louis, MO, USA), and counterstained with Hoechst 33342 (08168, Sigma-Aldrich, St. Louis, MO, USA) for 15 min. After fixation on glass slides, the oocytes were observed with laser scanning confocal microscope (TCS SP8; Leica Microsystems, Wetzlar, Germany). To detect reactive oxygen species (ROS) levels, oocytes were incubated with 10 µM 2′,7′-dichlorodihydrofluorescein diacetate (H2DCFDA) for 15 min at 37 °C. MitoTracker Red CMXRos (M7512; Thermo Fisher Scientific, Waltham, MA, USA) was used to detect mitochondria by incubating oocytes with the dye at 20 °C for 15 min. MitoSOX Red CMXRos (M36008; Thermo Fisher Scientific, Waltham, MA, USA) was used for mitochondrial detection by incubating oocytes with the dye at 37 °C for 20 min. Mitochondrial membrane potential was assessed using the JC-1 Assay Kit (ab113850, Abcam, Cambridge, UK). All images were taken with consistent settings and analyzed with ImageJ software (1.54f, National Institutes of Health, Bethesda, MD, USA).

2.7 Electron Microscopy

Transmission electron microscopy (TEM) was conducted using an average of 5 oocytes per group, with each group consisting of three biological replicates. Oocytes were fixed using electron microscopy fixative (G1102; Servicebio, Wuhan, China) and pre-embedded in agarose. This was followed by a series of steps including fixation, dehydration at room temperature, resin infiltration and embedding, polymerization, ultrathin sectioning on an ultramicrotome, and staining with uranyl acetate and lead citrate. Samples were then scanned with TEM, and images were captured for further analysis. The mitochondrial ultrastructure was assessed through electron micrographs at 40,000× magnification.

2.8 Carbonyl-cyanide-p-trifluoro-methoxy-phenylhydrazone (FCCP) Supplementation

The mitochondrial oxidative phosphorylation FCCP (HY-100410, MCE, Shanghai, China) was dissolved in DMSO (D4540, Sigma-Aldrich, St. Louis, MO, USA) and diluted to 200 nM in CZB medium.

2.9 RNA Isolation and Real-time Quantitative Polymerase Chain Reaction (RT-PCR)

Total oocyte RNA was isolated using the Arcturus PicoPure RNA Isolation Kit (Thermo Fisher, Waltham, MA, USA), and the RNA concentration was determined spectrophotometrically at 260/280 nm. RNA was reverse transcribed using the PrimeScript RT Master Mix (RR036B, TaKaRa, Dalian, China). Real-time fluorescence quantitative PCR was performed with SYBR Green Mix (740703, TaKaRa, Dalian, China). Primer sequences are referenced in **Supplementary Table 1**. *Hprt* was used as an internal control for quantifying gene expression. The specific qPCR parameters were 95 °C for 30 seconds, followed by 40 cy-

cles of 95 °C for 3 seconds and 60 °C for 30 seconds. This was followed by 15 seconds at 95 °C, 1 minute at 60 °C, and a final 15 seconds at 95 °C.

2.10 Chromosome Spreading

The zona pellucida was removed from the oocytes using 5% hydrochloric acid. Then the oocytes were quickly transferred to M2 medium and washed three times. To loosen the chromosomes, 1% potassium chloride was used to treat the oocytes for 3–5 min at room temperature. Then the oocytes were fixed on slides with a 1% PFA solution containing 0.15% Triton X-100 and 3 mM dithiothreitol (10197777001; Sigma-Aldrich). They were blocked in 3% BSA for 1 h. After staining the oocytes with CREST (1:200, sc-515827, Santa Cruz Biotechnology, Dallas, TX, USA) and Hoechst 33342 (1:1000), they were examined and counted using a confocal laser scanning microscope (TCS SP8; Leica).

2.11 Statistical Analyses

Values are shown as the mean ± standard error of the mean (SEM) from at least three independent experiments, and were analyzed with one-way analysis of variance using the GraphPad software (Version 8.0.2, GraphPad Software Inc., San Diego, CA, USA). Significance was accepted at $p \leq 0.05$.

3. Results

3.1 DHEA-induced PCOS Mice Exhibit Decreased TMAO Levels

We utilized DHEA to induce the PCOS mouse model (Fig. 1A). DHEA-induced PCOS mice showed significantly elevated plasma DHEA and testosterone levels (Fig. 1B,C), while plasma TMAO level were significantly decreased (Fig. 1D). FMO3, a key enzyme in the hepatic TMAO synthesis and sensitive to androgen levels, was measured in liver. The results demonstrated that FMO3 levels were significantly reduced in the PCOS group (Fig. 1E). To further explore the relationship between TMAO and PCOS, a 30-day TMAO supplementation was administered to PCOS mice. A control receiving only TMAO was set up to exclude its independent effects (Fig. 1A). The estrous cycles were recorded for four groups. PCOS mice lost the estrous cycle, but TMAO supplementation significantly rescued this phenomenon. Additionally, TMAO supplementation alone did not affect the estrous cycle (Fig. 1F). Based on these results, we propose that TMAO supplementation may improve estrous suppression in PCOS mice.

3.2 TMAO Improves Ovarian Function in PCOS Mice

We explored the effect of TMAO supplementation on PCOS-inducing reduction in the ovarian reserve. The ovarian morphology of PCOS mice was significantly smaller in size, lighter in color, and had a reduced vascular supply compared with the control group, TMAO supplementation reversed this change (Fig. 2A). The ovarian index (ovarian weight/body weight) in PCOS mice was significantly lower than control group. TMAO could mitigate the decline in ovarian indices, but there was no statistically significant difference (Fig. 2B). To further compare follicles development at all levels in the ovary, we performed serial sections of ovarian tissues. As observed in the H&E staining, in the ovarian tissues, PCOS group exhibited a large number of cystic follicles and significantly reduced antral follicles compared to the control group (Fig. 2C,D). Treating PCOS mice with TMAO, the increase in cystic follicles was ameliorated. Meanwhile, the decrease in antral follicles was also restored (Fig. 2C,D). These results indicated that TMAO supplementation could ameliorate ovulation disorders in PCOS mice.

3.3 TMAO Improves the Oocyte Maturation of PCOS Mice

To further elucidate the impact of TMAO on the meiotic progression of PCOS oocytes, we observed the ability of the oocyte to mature. First, we harvested MII oocytes from each group. At the same time, the average number and the rate of fragmented oocytes was counted. The results showed a notable increase in fragmented oocytes numbers and a lower MII oocyte acquisition rates within PCOS group. Supplementation of TMAO mitigates these changes (Fig. 3A–C). Second, we isolated GV oocytes from four groups and induced their maturation *in vitro* (Fig. 3D). The GV breakdown progression in PCOS oocytes was notably slower than in the NC and TMAO groups, yet it recovered with TMAO treatment (Fig. 3E). Our findings underscored a delayed entry of oocytes into the M phase in PCOS mice. Following 12 h of *in vitro* culture, the first polar body (PB1) extrusion rate was substantially lower in PCOS oocytes compared to both the NC and TMAO groups, but it recuperated in P+T oocytes (Fig. 3F). These findings collectively suggest that TMAO enhances maturation efficiency and rescues meiotic progression in PCOS oocytes.

3.4 Effect of TMAO on Developmental Potential of Oocytes in PCOS Mice

To determine whether the developmental potential of PCOS oocytes can improve by TMAO supplementation, we performed *in vitro* fertilization. Our results showed that the fertilization rate of PCOS oocytes was significantly lower compared to the NC and TMAO groups. As expected, TMAO supplementation increased the fertilization rate of PCOS oocytes (Fig. 4A,B). Then we monitored the early embryonic development and demonstrated that TMAO supplementation significantly improved the blastocyst formation rate of fertilized oocytes from PCOS mice (Fig. 4C). Next, morphologically normal blastocysts from each group were transplanted into pseudopregnant recipient females. Compared to the NC and TMAO groups, a significantly lower live birth number was observed in the PCOS group; however, TMAO supplementation partially improved this

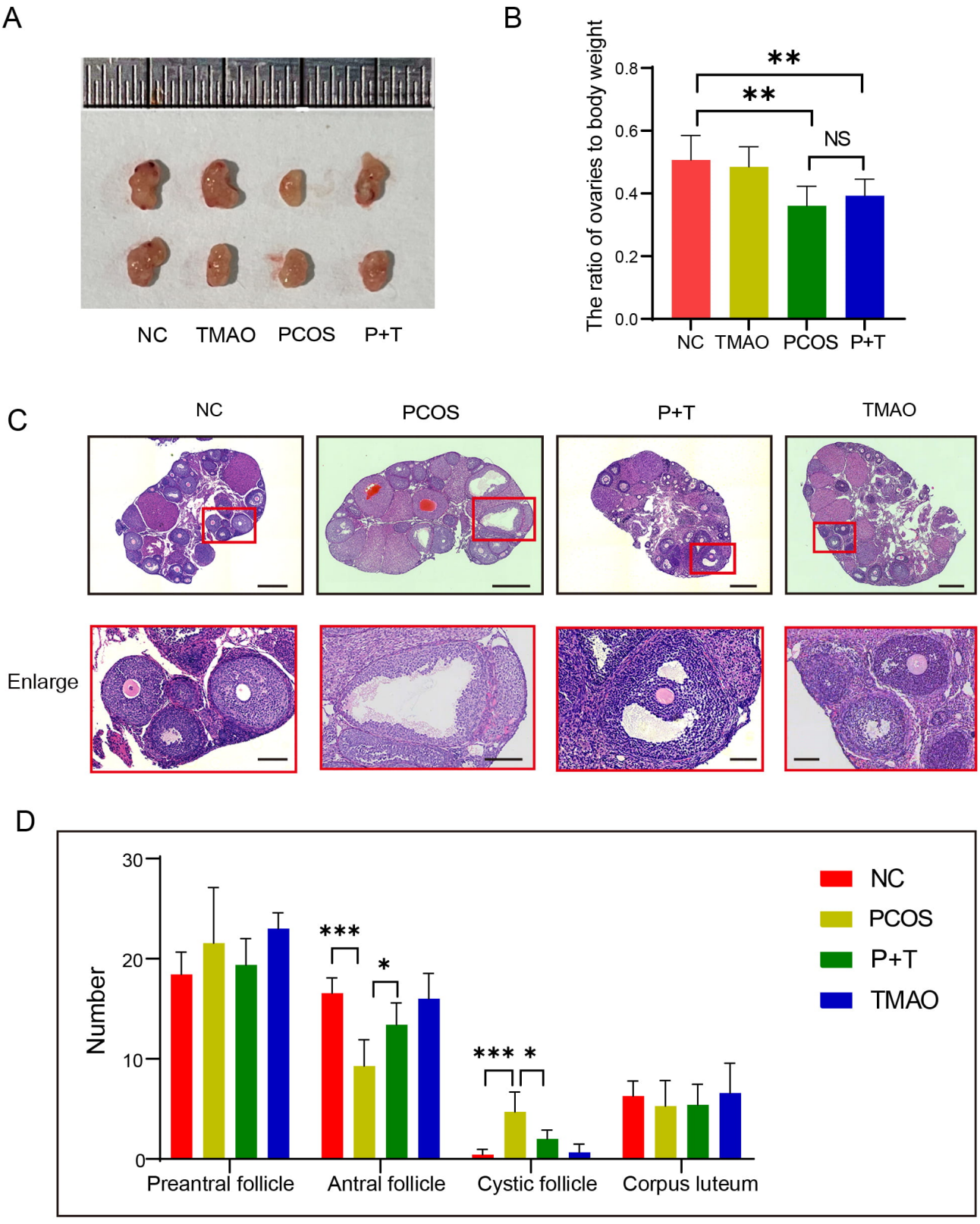

Fig. 2. The influence of TMAO on follicles population. (A) Representative image of ovary from NC, TMAO, PCOS and P+T group. (B) The rate of ovaries to body weight in four groups (n = 7, respectively). (C) Representative images of H&E staining of ovarian sections from NC, TMAO, PCOS and P+T mice. Scale bar: 250 µm, Scale bar of enlarged version: 50 µm. (D) Numbers of follicles at various stages in NC (n = 7), TMAO (n = 5), PCOS (n = 7) and P+T (n = 5) mice. Data are means ± SEM of at least three independent experiments. *$p < 0.05$, **$p < 0.01$, ***$p < 0.001$. H&E, hematoxylin and eosin; NS, no statistical differences.

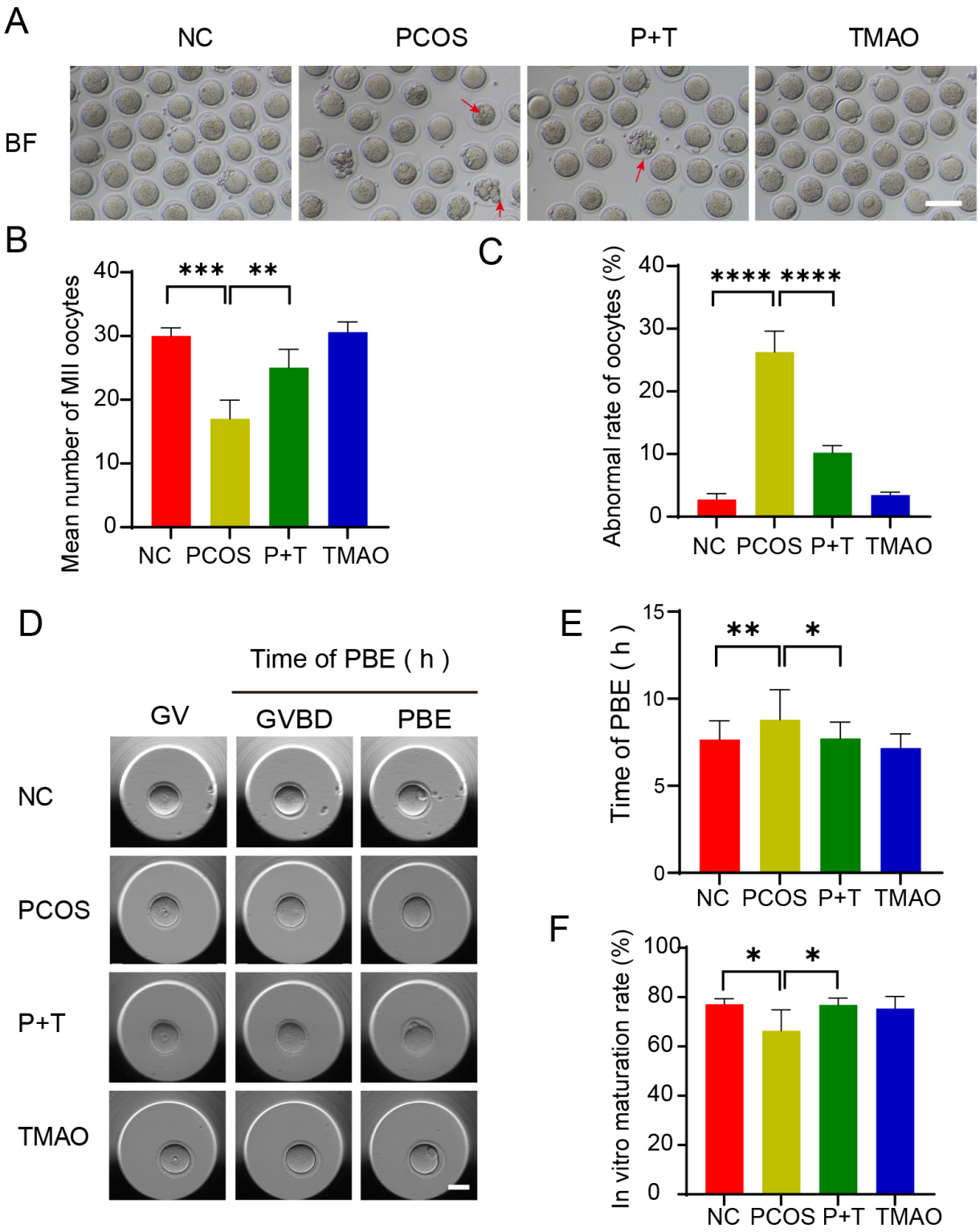

Fig. 3. Effect of TMAO on oocyte maturation in PCOS. (A) Representative image of MII oocytes from NC, PCOS, P+T and TMAO mice (n = 5). Red arrow: fragmented oocyte, Scale bar: 100 μm. (B) Average numbers of MII oocytes retrieved from NC, PCOS, P+T and TMAO mice (n = 8, respectively). (C) Abnormal rate of MII oocytes in four groups (n = 8, respectively). (D) Representative time-lapse images of NC, PCOS, P+T and TMAO, (n = 5, respectively) oocytes in indicated stage. Scale bar: 50 μm. (E) The incidence of PB1 was recorded in NC, PCOS, P+T and TMAO oocytes 12 hours after maturation *in vitro* (n = 5). (F) IVM rate of NC (n = 38), PCOS (n = 35), P+T (n = 40) and TMAO (n = 43) groups. Data are means ± SEM of at least three independent experiments. *$p < 0.05$, **$p < 0.01$, ***$p < 0.001$, ****$p < 0.0001$. PB1, first polar body; MII, metaphase II; GV, germinal vesicles; BF, blastocyst formation; PBE, polar body exclusion; GVBD, germinal vesicle breakdown.

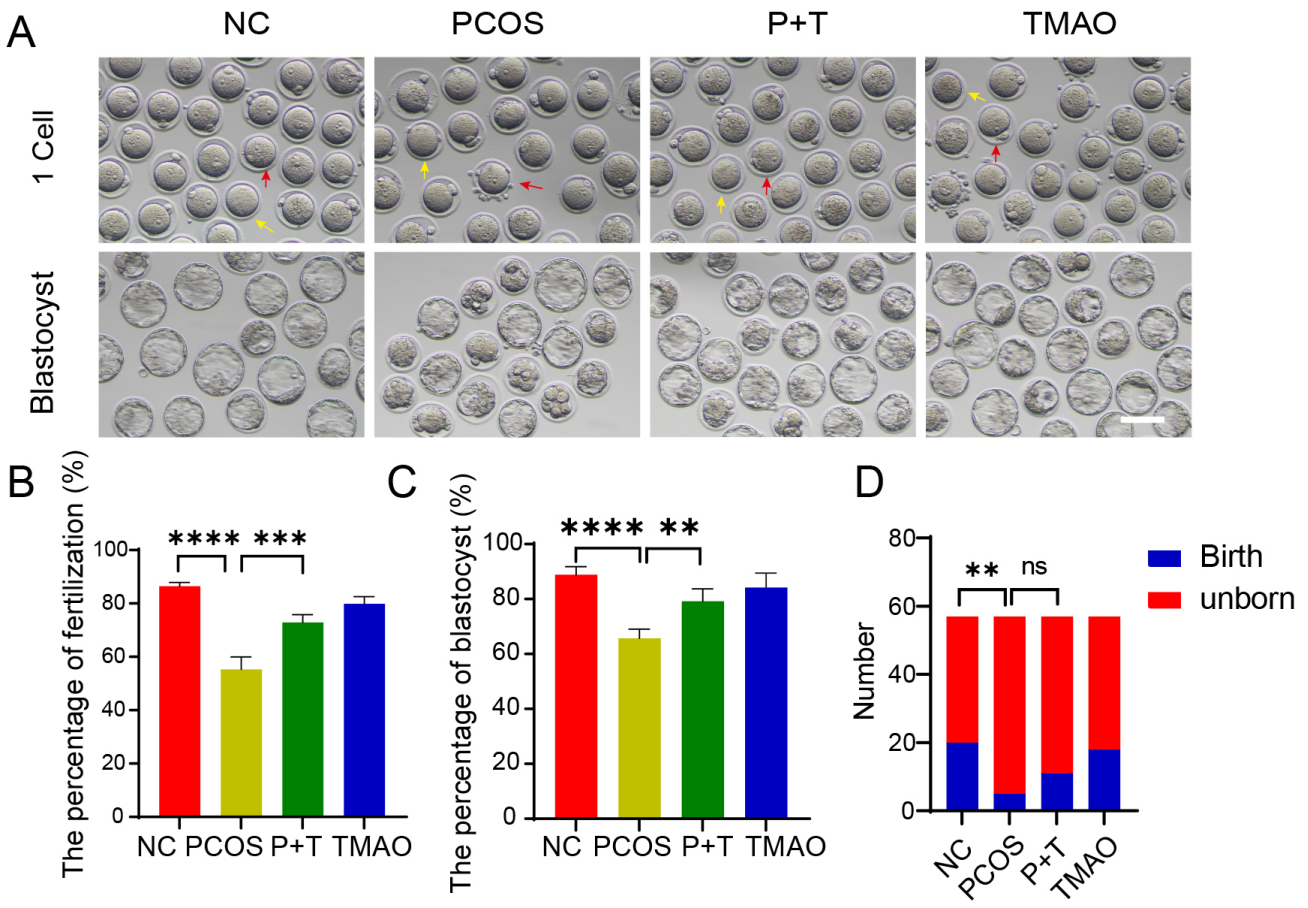

Fig. 4. Effects of TMAO on fertilization and embryo developmental potential. (A) Representative image of NC, PCOS, P+T and TMAO embryos in IVF process. Red arrow: embryo failed to fertilization, yellow arrow: embryo successed in IVF. Scale bar: 100 μm. (B,C) The fertilization rate and blastocyst rate of NC (n = 153), PCOS (n = 125), P+T (n = 141) and TMAO (n = 138) groups were detected. (D) The birth number after blastocyst transfer (n = 57, respectively) of mice from four groups (n = 6, respectively). Data are means ± SEM of at least three independent experiments. $^{**}p < 0.01$, $^{***}p < 0.001$, $^{****}p < 0.0001$, ns, no statistical differences; IVF, *in vitro* fertilization.

outcome (Fig. 4D). These results suggest that TMAO supplementation increases the fertilization ability and developmental potential of PCOS oocytes.

3.5 TMAO Reduces Chromosomal Spindle Defects and Aneuploidy Rate in PCOS Oocytes

Spindle assembly and chromosome alignment are critical indicators of oocyte quality. Therefore, we examined spindle/chromosome structure in MII oocytes. In the NC and TMAO-alone groups, a typical barrel-shaped spindle with well-aligned chromosomes was observed (Fig. 5A). However, oocytes from the PCOS group had a higher percentage of abnormal spindle organization and/or misaligned chromosomes (Fig. 5A–C). Next, we observed the spindle function of GV oocytes during maturation to MII oocytes *in vitro* and found that microtubule fiber non-attachment to the mitotic granules was more pronounced in the PCOS group. However, in the P+T group, the proportion of microtubule fiber attachment abnormalities rate was significantly reduced (Fig. 5D–F). Because impaired spindle/chromosome structure is usually coupled with aneuploidy, we analyzed the karyotype of MII oocytes through DNA sequencing. Quantitative comparisons revealed that the aneuploidy rate of oocytes in the PCOS group was higher compared to the control group, and TMAO supplementation was able to reduce the aneuploidy rate in the PCOS group. The abnormal aneuploidy rate of PCOS was 23.78%, and TMAO supplementation reduced it to 19% (Fig. 5G,H). Therefore, TMAO supplementation could reduce the rates of abnormal spindle/chromosome defects and aneuploidy in PCOS oocytes.

3.6 TMAO Suppresses Oxidative Stress in PCOS Oocytes

Excessive ROS level is a significant cause of decreased oocyte quality. Therefore, we assessed the ROS level using dichlorofluorescein (DCFH) staining. The results showed that ROS signals were significantly higher in PCOS oocytes compared to the NC and TMAO groups. By contrast, TMAO supplementation effectively reduced accumulated ROS in PCOS oocytes (Fig. 6A,B). Given

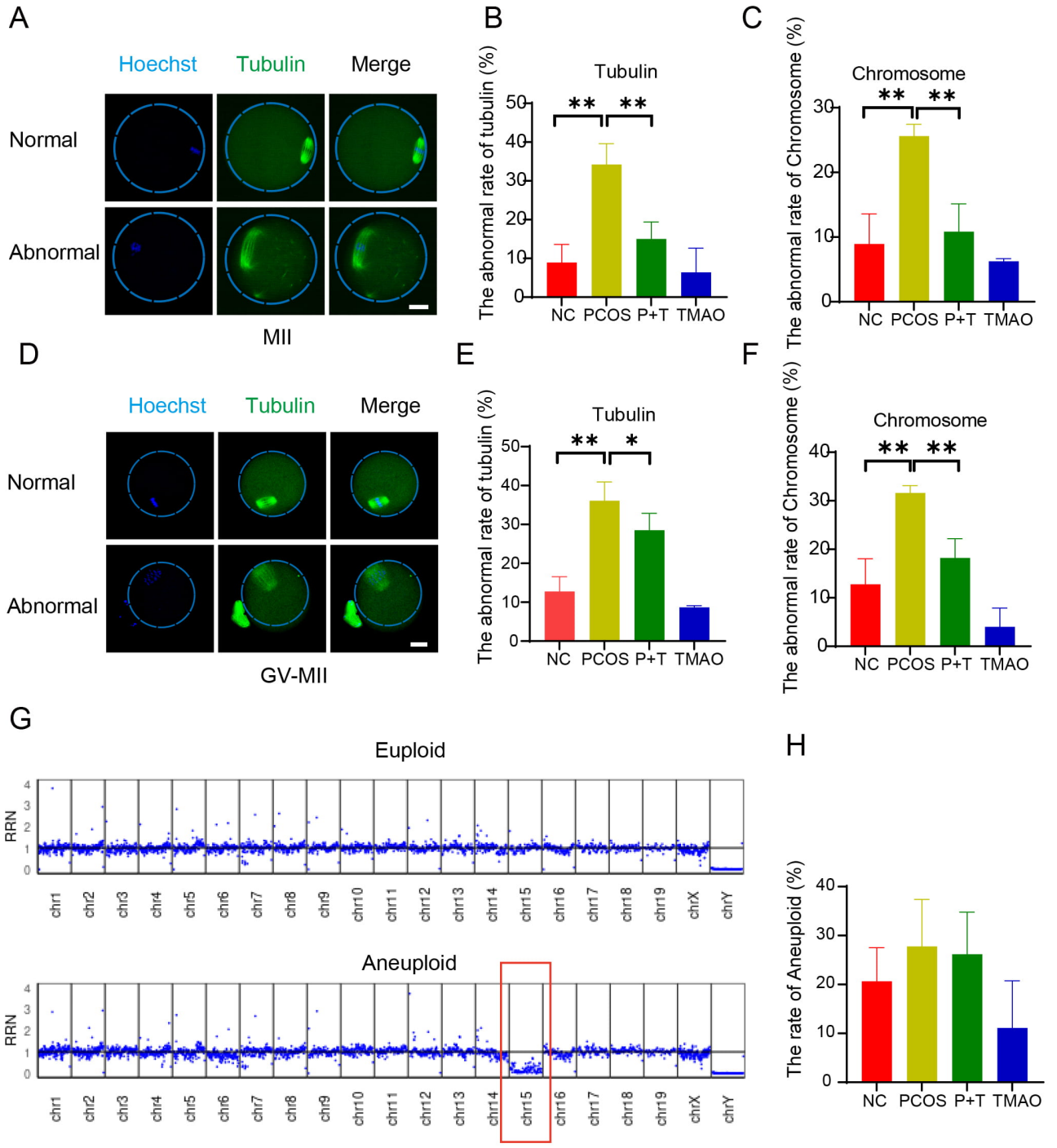

Fig. 5. Effect of TMAO supplementation on the spindle/chromosome structure and developmental potential of oocytes of PCOS mice. (A) Representative image of normal and abnormal spindle morphology and chromosome alignment in MII oocytes. Scale bar: 40 µm. (B,C) Aberrant spindle rates and misaligned chromosome rates of NC (n = 46), PCOS (n = 47), P+T (n = 47) and TMAO (n = 48) MII oocytes. (D) Representative images of normal and abnormal spindle morphology and chromosome alignment in GV-MII oocytes. Scale bar: 40 µm. (E,F) Aberrant spindle rates and misaligned chromosome rates of NC (n = 47), PCOS (n = 48), P+T (n = 43) and TMAO (n = 44). (G,H) Chromosomal ploidy detection of mature MII oocytes *in vivo* of NC (n = 19), PCOS (n = 18), P+T (n = 19), TMAO (n = 17). Data are means ± SEM of at least three independent experiments. *$p < 0.05$, **$p < 0.01$.

the central role of mitochondria in energy metabolism in oocytes, we used MitoSOX staining to measure mitochondrial ROS content and clarify the source of ROS in oocytes. The PCOS oocytes exhibited higher levels of mitochondrial ROS than those in the NC and TMAO groups, and this elevated level was reduced by TMAO supplementation

(Fig. 6C,D). These results suggest that TMAO supplementation reduces ROS levels in both the cytoplasm and mitochondria of PCOS oocytes.

3.7 TMAO Improves Mitochondrial Function of Oocytes in PCOS Mice

Mitochondrial function is closely related to ROS levels. Therefore, we assessed the distribution pattern of mitochondria using MitoTracker staining. In the NC and TMAO groups, mitochondria exhibited a typical distribution pattern, accumulating around the chromosomes and homogeneously distributed in the cytoplasm. However, in PCOS oocytes, many mitochondria partially or completely lost their peripheral chromosomal accumulation and showed absent or aggregated distribution in the cytoplasm (Fig. 7A,B). Quantitatively, more than 30% of mitochondria displayed abnormal distribution in PCOS oocytes, which was reduced to 13% with TMAO supplementation (Fig. 7B). We evaluated the mitochondrial membrane potential using JC-1 staining. The ratio of red to green signals was significantly weaker in PCOS oocytes compared to NC and TMAO oocytes but was reversed by TMAO supplementation (Fig. 7C,D). Additionally, we quantified the mitochondrial DNA (mtDNA) copy number. The PCOS group showed a significant decrease in mtDNA copy number compared to the NC and TMAO groups, but this was partially restored in the P+T group (Fig. 7E). We also examined the expression of key genes involved in mitochondrial function (cytochrome c oxidase subunit 5b [*Cox5b*], succinate dehydrogenase complex assembly factor 4 [*Sdhaf4*], solute carrier family 17 member 5, mitochondrial fission factor, and NADH: ubiquinone oxidoreductase core subunit S1), and found that *Cox5b* and *Sdhaf4* were downregulated in PCOS oocytes but restored to comparable levels with TMAO supplementation (Fig. 7F). Transmission emission microscopy showed that the mitochondria of PCOS oocytes exhibited loose membranes and cristae, narrow intermembrane spaces, and swollen vacuoles. In P+T oocytes, the mitochondrial ultrastructure was similar to that of NC and TMAO oocytes (Fig. 7G,H).

As the primary energy sources in oocytes, the mitochondria produce ATP via the oxidative phosphorylation (OXPHOS) pathway. Carbonyl-cyanide-p-trifluoromethoxy-phenylhydrazone (FCCP) is a highly effective uncoupler of mitochondrial OXPHOS. Next, we collected GV oocytes from the PCOS group. Then GV oocytes were treated with FCCP for 18 h. FCCP prevented the TMAO-induced reduction in ROS levels (Fig. 7I,J), spindle defects (Fig. 7K–M), PB1 extrusion time (**Supplementary Fig. 1A,B**), and IVM rate (**Supplementary Fig. 1C**). These observations suggest that TMAO improves the quality of PCOS oocytes through mitochondrial protection.

4. Discussion

Hyperandrogenism and ovulatory dysfunction are typical clinical manifestations of PCOS. This process is often accompanied by significant elevation of ROS [18], which leads to chronic inflammation throughout the body, including ovarian tissue [14,19,20]. The main source of ROS in organisms is the mitochondria. Several studies have shown that mitochondrial function is dysfunctional in patients with PCOS [13,21–24], which is related to mtDNA replication and mitochondrial OXPHOS efficiency. The elevated ROS levels in PCOS oocytes can disrupt DNA repair proteins and spindle structure, resulting in aneuploidy and reduced developmental potential [25]. Some therapy methods, such as vitamin C [26], metformin [27,28], and inositol [29,30], were used to ameliorate high oxidative stress levels in patients with PCOS. However, the optimal dosage, duration, and effectiveness in PCOS management are still subject to ongoing research [31,32]. Therefore, the development of therapies with the potential to improve oocyte quality in patients with PCOS has a considerable practical application value in ART. In this experiment, we established the PCOS mouse model using DHEA. We found that the PCOS mice showed elevated plasma androgens and reduced levels of plasma TMAO.

TMAO is a metabolite produced by intestinal flora and serves as an important indicator of the body's metabolic state; however, its role in oocytes remains unclear. Previous study has found that TMAO levels decrease with increasing blood androgen levels, which is caused by a decrease in hepatic FMO3 expression [33]. Therefore, we supplemented TMAO to DHEA-induced PCOS mice and observed its effects. We found that follicular development, ovulation, and oocyte maturation were impaired in PCOS mice. TMAO supplementation increased the number of antral follicles, ovulating oocytes, and mature oocytes to some extent, while reducing oocyte fragmentation. Additionally, TMAO increased the maturation rate of PCOS oocytes by promoting nuclear and cytoplasmic maturation. TMAO restored spindle/chromosome structure and kinetochore-microtubule attachment, thereby maintaining normal aneuploidy rates and nuclear maturation in PCOS oocytes. In addition, early embryonic development was promoted.

During oocyte maturation, the mtDNA copy number spikes and the distribution of mitochondria change significantly [34]. As oocyte maturation requires a large amount of ATP for continuous transcription and translation, an appropriate number of functional mitochondria is crucial [35]. We examined intra-oocyte and mitochondrial ROS levels and found that TMAO significantly reduced ROS levels. Electron microscopy examination of mitochondrial morphology and membrane potential levels revealed that the effects of TMAO on PCOS may be mediated by improvements in mitochondrial function. This is consistent with the idea that ROS production in the PCOS state is di-

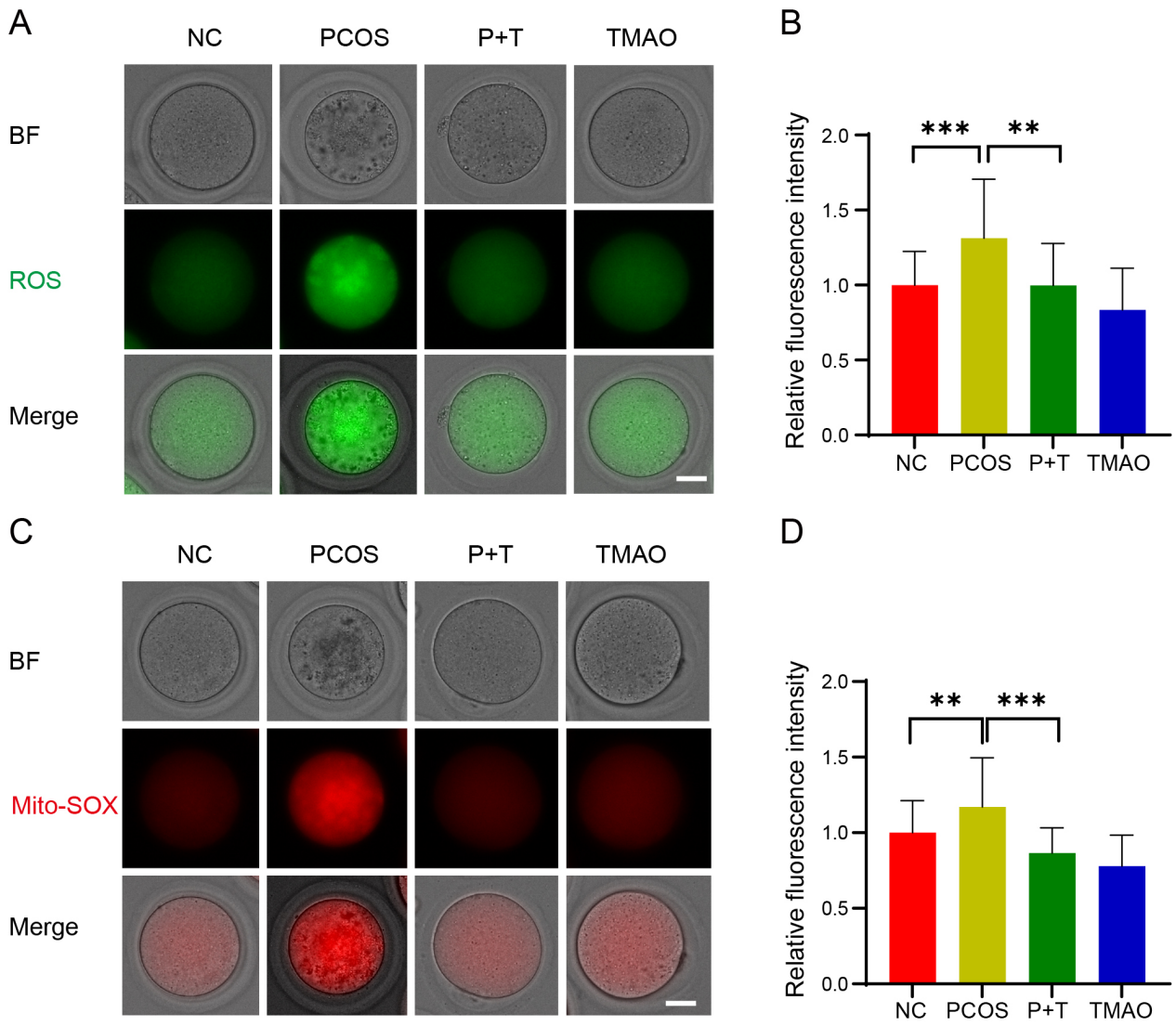

Fig. 6. Effect of TMAO supplementation on ROS levels in oocytes. (A) Representative image of ROS expression detected by DCFH staining of each group, Scale bar: 40 μm. (B) The fluorescence intensity of ROS signals was measured in NC (n = 35), PCOS (n = 33), P+T (n = 33) and TMAO (n = 36) groups. (C) Detection of mitochondrial oxidative stress levels. Representative images of Mito-SOX fluorescence of each group. Scale bar: 40 μm. (D) The fluorescence intensity of Mito-SOX signals was measured in NC (n = 32), PCOS (n = 28), P+T (n = 30) and TMAO (n = 34) groups. Data are means ± SEM of at least three independent experiments. $^{**}p < 0.01$, $^{***}p < 0.001$. ROS, reactive oxygen species; DCFH, dichlorofluorescein.

rectly related to mtDNA replication and mitochondrial OXPHOS efficiency [19,36]. Reduced mitochondrial membrane potential and impaired predict ROS accumulation and apoptosis in PCOS oocytes, contributing to ovarian hypoplasia in PCOS [15,37]. Subsequent analyses of mitochondrial distribution, ATP content, and mitochondrial membrane potential showed that TMAO reversed PCOS-induced mitochondrial dysfunction in oocytes. Our data suggest that TMAO supplementation is effective in eliminating excess ROS and restoring mitochondrial function in PCOS oocytes. Additionally, ROS accumulation can affect spindle function and microtubule structure, which are related to the haploid rate and developmental potential of oocytes [38,39].

However, in addition to hyperandrogenemia, the disease progression of PCOS patients encompasses insulin resistance and chronic inflammation. The effect of TMAO to improve mitochondrial function and oocyte quality would benefit PCOS patients undergoing ART treatment. Nevertheless, comprehensive management of systemic oxidative stress in PCOS patients demands further investigation.

5. Conclusions

In summary, our experiments demonstrated that TMAO reduced ROS levels while improving spindle/chromosome structure and kinetochore-microtubule attachment in PCOS oocytes. We provide evidence that

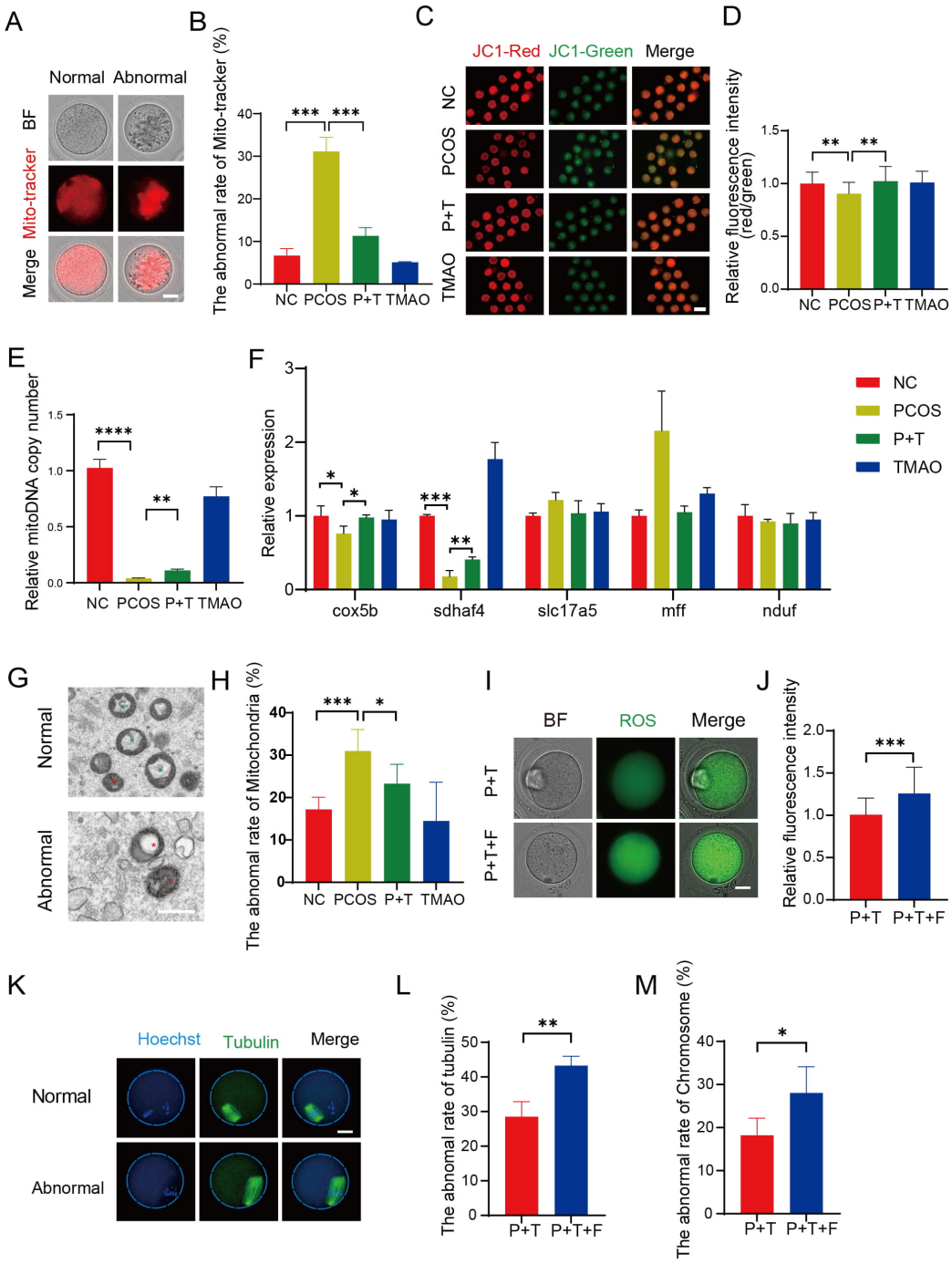

Fig. 7. Effect of TMAO on mitochondrial function in PCOS oocytes. (A) Representative image of mitochondrial distribution in oocytes detected with Mito-tracker. Scale bar: 40 μm. (B) The abnormal rate of Mito-tracker in each group (n = 3). (C) Representative images of JC-1 fluorescence of each group. Scale bar: 40 μm. (D) The fluorescence intensity of JC-1 signals was measured in NC (n = 32), PCOS (n = 28), P+T (n = 30) and TMAO (n = 34) groups. (E) The relative copy number of mitoDNA in four groups (n = 3). (F) The relative expression level of gene *cox5b*, *sdhaf4*, *slc17a5*, *mff* and *nduf* (n = 3, respectively). (G) The representative images of normal and abnormal mitochondria. Scale bar: 100 μm. Red * : abnormal mitochondria. Green * : normal mitochondria. (H) Proportion of normal and abnormal mitochondria in NC (n = 216), PCOS (n = 266), P+T (n = 324), and TMAO (n = 217) groups. (I,J) The fluorescence intensity of ROS signals in P+T (n = 21) and PCOS+TMAO+FCCP (P+T+F) (n = 22) groups. Scale bar: 20 μm. (K) Representative image of normal and abnormal spindle morphology in oocytes after *in vitro* maturation. Scale bar: 40 μm. (L,M) Normal and abnormal spindle and chromosome morphology and number in oocytes after *in vitro* maturation of PCOS+TMAO (n = 43) and P+T+F (n = 54) groups. The data are means ± SEM of at least three independent experiments. *$p < 0.05$, **$p < 0.01$, ***$p < 0.001$, ****$p < 0.0001$. FCCP, carbonyl-cyanide-p-trifluoro-methoxy-phenylhydrazone; mtDNA, mitochondrial DNA.

TMAO improves PCOS oocyte quality by promoting oocyte maturation, maintaining aneuploidy, and enhancing fertility. Our work demonstrates the potential and experimental basis for using TMAO to improve fertility and ART efficiency in patients with PCOS.

Abbreviations

ART, assisted reproductive technology; TMAO, trimethylamine N-oxide; PCOS, polycystic ovary syndrome; DHEA, dehydroepiandrosterone; ROS, reactive oxygen species; SCFAs, short-chain fatty acids; FMO3, flavin-containing monooxygenase 3; ICR, Institute of Cancer Research; NC, Normal control; LC-MS/MS, Liquid chromatography–tandem mass spectrometry; GV, germinal vesicles; PMSG, pregnant mare serum gonadotropin; CO_2, carbon dioxide; IVM, *in vitro* maturation; MII, metaphase II; HTF, Human Tubal Fluid; hCG, human chorionic gonadotrophin; PVA, polyvinyl alcohol; TEM, transmission electron microscopy; FCCP, carbonyl-cyanide-p-trifluoromethoxy-phenylhydrazone; RT-PCR, real-time quantitative polymerase chain reaction; SEM, standard error of the mean; PB1, first polar body.

Availability of Data and Materials

The datasets used and/or analyzed during the current study are available from the corresponding authors on reasonable request.

Author Contributions

JYHua and JYL conceptualized the study design. JYHou, YT, XML, CL, LZ, XRL and ZXX wrote the initial drafts of the manuscript. JYHua and YT: Designed the experiments; Performed the experiments; Collected and analyzed data. Made figures; XML, LZ, CL, XRL and ZXX: Participated in experiments; Provided technical support. JYHou and JYL: Collected and analyzed data; wrote the paper; Supervision, and Funding acquisition. All authors contributed to editorial changes in the manuscript. All authors have read and approved the final manuscript. All authors have participated sufficiently in the work and agreed to be accountable for all aspects of the work.

Ethics Approval and Consent to Participate

The animal study protocol was approved by the Ethics Committee of Chongqing Medical University (Title of project: Mechanisms of TMAO in affecting the quality and developmental potential of PCOS oocytes; Approved number: IACUC-CQMU-2023-0152; Date of approval: 2023-06-13) for studies involving animals. The reporting of this study conforms to ARRIVE 2.0 guidelines.

Acknowledgment

Not applicable.

Funding

The study was supported by National Key R&D Program of China, 2023YFC2705400; National Natural Science Foundation of China, No.82101711; Chongqing Postdoctoral Scientific Research Special Funding Project, No. 2022CQBSHTB1028; Beijing Health Promotion Association, Research Project for Young and Middle-aged Doctors in Reproductive Field, BJHPA-2021-SHZHYXZHQNYJ-004; Open Project of Chongqing Key Laboratory of Human Embryo Engineering, No.2020KFKT006. The Scientific and Technological Research Program of Chongqing Medical and Pharmaceutical College, No. ygzrc2023106.

Conflict of Interest

The authors declare no conflict of interest.

Supplementary Material

Supplementary material associated with this article can be found, in the online version, at https://doi.org/10.31083/FBL38078.

References

[1] Yu O, Christ JP, Schulze-Rath R, Covey J, Kelley A, Grafton J, *et al*. Incidence, prevalence, and trends in polycystic ovary syndrome diagnosis: A United States population-based study from 2006 to 2019. American Journal of Obstetrics and Gynecology. 2023; 229: 39.e1–39.e12. https://doi.org/10.1016/j.ajog.2023.04.010.

[2] Witchel SF, Oberfield SE, Peña AS. Polycystic Ovary Syndrome: Pathophysiology, Presentation, and Treatment With Emphasis on Adolescent Girls. Journal of the Endocrine Society. 2019; 3: 1545–1573. https://doi.org/10.1210/js.2019-00078.

[3] Rotterdam ESHRE/ASRM-Sponsored PCOS consensus workshop group. Revised 2003 consensus on diagnostic criteria and long-term health risks related to polycystic ovary syndrome (PCOS). Human Reproduction (Oxford, England). 2004; 19: 41–47. https://doi.org/10.1093/humrep/deh098.

[4] Gupta M, Yadav R, Mahey R, Agrawal A, Upadhyay A, Malhotra N, *et al*. Correlation of body mass index (BMI), anti-mullerian hormone (AMH), and insulin resistance among different polycystic ovary syndrome (PCOS) phenotypes - a cross-sectional study. Gynecological Endocrinology: The Official Journal of the International Society of Gynecological Endocrinology. 2019; 35: 970–973. https://doi.org/10.1080/09513590.2019.1613640.

[5] Kotlyar AM, Seifer DB. Women with PCOS who undergo IVF: a comprehensive review of therapeutic strategies for successful outcomes. Reproductive Biology and Endocrinology: RB&E. 2023; 21: 70. https://doi.org/10.1186/s12958-023-01120-7.

[6] Qi X, Yun C, Sun L, Xia J, Wu Q, Wang Y, *et al*. Gut microbiota-bile acid-interleukin-22 axis orchestrates polycystic ovary syndrome. Nature Medicine. 2019; 25: 1225–1233. https://doi.org/10.1038/s41591-019-0509-0.

[7] Rodriguez Paris V, Wong XYD, Solon-Biet SM, Edwards MC, Aflatounian A, Gilchrist RB, *et al*. The interplay between PCOS pathology and diet on gut microbiota in a mouse model. Gut Microbes. 2022; 14: 2085961. https://doi.org/10.1080/19490976.2022.2085961.

[8] Aron-Wisnewsky J, Warmbrunn MV, Nieuwdorp M, Clément K. Metabolism and Metabolic Disorders and the Microbiome: The Intestinal Microbiota Associated With Obesity, Lipid Metabolism, and Metabolic Health-Pathophysiology and Thera-

peutic Strategies. Gastroenterology. 2021; 160: 573–599. https://doi.org/10.1053/j.gastro.2020.10.057.

[9] Gatarek P, Kaluzna-Czaplinska J. Trimethylamine N-oxide (TMAO) in human health. EXCLI Journal. 2021; 20: 301–319. https://doi.org/10.17179/excli2020-3239.

[10] Roberts AB, Gu X, Buffa JA, Hurd AG, Wang Z, Zhu W, *et al*. Development of a gut microbe-targeted nonlethal therapeutic to inhibit thrombosis potential. Nature Medicine. 2018; 24: 1407–1417. https://doi.org/10.1038/s41591-018-0128-1.

[11] Orozco Cabral JA, Lee PC, Wang S, Wang Y, Zhang Y, Comizzoli P, *et al*. The Effect of Choline Salt Addition to Trehalose Solution for Long-Term Storage of Dried and Viable Nuclei from Fully Grown Oocytes. Bioengineering (Basel, Switzerland). 2023; 10: 1000. https://doi.org/10.3390/bioengineering10091000.

[12] Huang JYJ, Chen HY, Tan SL, Chian RC. Effect of choline-supplemented sodium-depleted slow freezing versus vitrification on mouse oocyte meiotic spindles and chromosome abnormalities. Fertility and Sterility. 2007; 88: 1093–1100. https://doi.org/10.1016/j.fertnstert.2006.12.066.

[13] Murri M, Luque-Ramírez M, Insenser M, Ojeda-Ojeda M, Escobar-Morreale HF. Circulating markers of oxidative stress and polycystic ovary syndrome (PCOS): a systematic review and meta-analysis. Human Reproduction Update. 2013; 19: 268–288. https://doi.org/10.1093/humupd/dms059.

[14] Liu Y, Yu Z, Zhao S, Cheng L, Man Y, Gao X, *et al*. Oxidative stress markers in the follicular fluid of patients with polycystic ovary syndrome correlate with a decrease in embryo quality. Journal of Assisted Reproduction and Genetics. 2021; 38: 471–477. https://doi.org/10.1007/s10815-020-02014-y.

[15] Zhang Q, Ren J, Wang F, Pan M, Cui L, Li M, *et al*. Mitochondrial and glucose metabolic dysfunctions in granulosa cells induce impaired oocytes of polycystic ovary syndrome through Sirtuin 3. Free Radical Biology & Medicine. 2022; 187: 1–16. https://doi.org/10.1016/j.freeradbiomed.2022.05.010.

[16] Gao Y, Zou Y, Wu G, Zheng L. Oxidative stress and mitochondrial dysfunction of granulosa cells in polycystic ovarian syndrome. Frontiers in Medicine. 2023; 10: 1193749. https://doi.org/10.3389/fmed.2023.1193749.

[17] Lin X, Zhang Y, He X, Chen Y, Chen N, Liu J, *et al*. The Choline Metabolite TMAO Inhibits NETosis and Promotes Placental Development in GDM of Humans and Mice. Diabetes. 2021; 70: 2250–2263. https://doi.org/10.2337/db21-0188.

[18] ESHRE Guideline Group on Good Practice in IVF Labs, De los Santos MJ, Apter S, Coticchio G, Debrock S, Lundin K, *et al*. Revised guidelines for good practice in IVF laboratories (2015). Human Reproduction (Oxford, England). 2016; 31: 685–686. https://doi.org/10.1093/humrep/dew016.

[19] Zhao H, Zhao Y, Li T, Li M, Li J, Li R, *et al*. Metabolism alteration in follicular niche: The nexus among intermediary metabolism, mitochondrial function, and classic polycystic ovary syndrome. Free Radical Biology & Medicine. 2015; 86: 295–307. https://doi.org/10.1016/j.freeradbiomed.2015.05.013.

[20] Masjedi F, Keshtgar S, Agah F, Karbalaei N. Association Between Sex Steroids and Oxidative Status with Vitamin D Levels in Follicular Fluid of Non-obese PCOS and Healthy Women. Journal of Reproduction & Infertility. 2019; 20: 132–142.

[21] Zhang R, Liu H, Bai H, Zhang Y, Liu Q, Guan L, *et al*. Oxidative stress status in Chinese women with different clinical phenotypes of polycystic ovary syndrome. Clinical Endocrinology. 2017; 86: 88–96. https://doi.org/10.1111/cen.13171.

[22] Wang H, Ruan X, Li Y, Cheng J, Mueck AO. Oxidative stress indicators in Chinese women with PCOS and correlation with features of metabolic syndrome and dependency on lipid patterns. Archives of Gynecology and Obstetrics. 2019; 300: 1413–1421. https://doi.org/10.1007/s00404-019-05305-7.

[23] Mohammadi M. Oxidative Stress and Polycystic Ovary Syndrome: A Brief Review. International Journal of Preventive Medicine. 2019; 10: 86. https://doi.org/10.4103/ijpvm.IJPVM_576_17.

[24] Patel S. Polycystic ovary syndrome (PCOS), an inflammatory, systemic, lifestyle endocrinopathy. The Journal of Steroid Biochemistry and Molecular Biology. 2018; 182: 27–36. https://doi.org/10.1016/j.jsbmb.2018.04.008.

[25] Rottenberg H, Hoek JB. The Mitochondrial Permeability Transition: Nexus of Aging, Disease and Longevity. Cells. 2021; 10: 79. https://doi.org/10.3390/cells10010079.

[26] Heidari H, Hajhashemy Z, Saneei P. A meta-analysis of effects of vitamin E supplementation alone and in combination with omega-3 or magnesium on polycystic ovary syndrome. Scientific Reports. 2022; 12: 19927. https://doi.org/10.1038/s41598-022-24467-0.

[27] Bai B, Chen H. Metformin: A Novel Weapon Against Inflammation. Frontiers in Pharmacology. 2021; 12: 622262. https://doi.org/10.3389/fphar.2021.622262.

[28] Sam S, Ehrmann DA. Metformin therapy for the reproductive and metabolic consequences of polycystic ovary syndrome. Diabetologia. 2017; 60: 1656–1661. https://doi.org/10.1007/s00125-017-4306-3.

[29] Dinicola S, Minini M, Unfer V, Verna R, Cucina A, Bizzarri M. Nutritional and Acquired Deficiencies in Inositol Bioavailability. Correlations with Metabolic Disorders. International Journal of Molecular Sciences. 2017; 18: 2187. https://doi.org/10.3390/ijms18102187.

[30] Unfer V, Facchinetti F, Orrù B, Giordani B, Nestler J. Myo-inositol effects in women with PCOS: a meta-analysis of randomized controlled trials. Endocrine Connections. 2017; 6: 647–658. https://doi.org/10.1530/EC-17-0243.

[31] Zeber-Lubecka N, Ciebiera M, Hennig EE. Polycystic Ovary Syndrome and Oxidative Stress-From Bench to Bedside. International Journal of Molecular Sciences. 2023; 24: 14126. https://doi.org/10.3390/ijms241814126.

[32] Siddiqui S, Mateen S, Ahmad R, Moin S. A brief insight into the etiology, genetics, and immunology of polycystic ovarian syndrome (PCOS). Journal of Assisted Reproduction and Genetics. 2022; 39: 2439–2473. https://doi.org/10.1007/s10815-022-02625-7.

[33] Bennett BJ, de Aguiar Vallim TQ, Wang Z, Shih DM, Meng Y, Gregory J, *et al*. Trimethylamine-N-oxide, a metabolite associated with atherosclerosis, exhibits complex genetic and dietary regulation. Cell Metabolism. 2013; 17: 49–60. https://doi.org/10.1016/j.cmet.2012.12.011.

[34] Kirillova A, Smitz JEJ, Sukhikh GT, Mazunin I. The Role of Mitochondria in Oocyte Maturation. Cells. 2021; 10: 2484. https://doi.org/10.3390/cells10092484.

[35] Van Blerkom J. Mitochondrial function in the human oocyte and embryo and their role in developmental competence. Mitochondrion. 2011; 11: 797–813. https://doi.org/10.1016/j.mito.2010.09.012.

[36] Dong XC, Liu C, Zhuo GC, Ding Y. Potential Roles of mtDNA Mutations in PCOS-IR: A Review. Diabetes, Metabolic Syndrome and Obesity: Targets and Therapy. 2023; 16: 139–149. https://doi.org/10.2147/DMSO.S393960.

[37] Zhao S, Heng N, Wang H, Wang H, Zhang H, Gong J, *et al*. Mitofusins: from mitochondria to fertility. Cellular and Molecular Life Sciences: CMLS. 2022; 79: 370. https://doi.org/10.1007/s00018-022-04386-z.

[38] Sasaki H, Hamatani T, Kamijo S, Iwai M, Kobanawa M, Ogawa S, *et al*. Impact of Oxidative Stress on Age-Associated Decline in Oocyte Developmental Competence. Frontiers in Endocrinology. 2019; 10: 811. https://doi.org/10.3389/fendo.2019.00811.

[39] Cao B, Qin J, Pan B, Qazi IH, Ye J, Fang Y, *et al*. Oxidative Stress and Oocyte Cryopreservation: Recent Advances in Mitigation Strategies Involving Antioxidants. Cells. 2022; 11: 3573. https://doi.org/10.3390/cells11223573.